COMPARISON OF URBAN/RURAL COUNTER AND NET RADIATION AT NIGHT

T. R. OKE

Dept. of Geography, University of British Columbia, Vancouver, B.C.

and

R. F. FUGGLE

Dept. of Environmental Studies, University of the Witwatersrand, Johannesburg, S. Africa

(Received 16 June, 1971)

Abstract. Comparison of incoming long-wave radiation at night in urban and rural locations has been achieved via direct measurements. Counter radiation and air temperature were continuously monitored during automobile traverses across the Island of Montreal on clear nights. Results show that urban counter radiation values are consistently slightly higher than rural values. The cross-Montreal radiation profiles closely parallel the form of the urban heat island.

Comparison of measured counter radiation with that computed from empirical equations shows a fair absolute agreement, but important urban/rural differences. Analysis of these differences suggests that the urban counter radiation anomaly is explainable on the basis of the vertical temperature structure of the city alone, without need to consider emissivity changes brought about by air pollution. This suggests that the increased counter radiation is a result, not a cause of the urban heat island.

Estimates of net long-wave radiation show only small urban/rural differences. Thus the increased counter radiation appears to be nullified by an increased emission from the warmer city surface.The study indicates that radiative exchanges probably play a minor role in nocturnal urban/rural surface energy balance differences.

1. Introduction

Our understanding of the most basic energy exchanges necessary for a sound climatology is almost totally lacking for the urban environment. Even the workings of the fundamental radiative components remain largely speculative. At present there is a considerable drive to produce workable atmospheric dispersion models which take account of the complexities of the urban interface. There is, however, evidence that our ability to model has outstripped the physical data base (e.g., Stern, 1970). This leads to the use of unfounded assumptions regarding input data and boundary conditions, and little chance of 'validating' the output against the real-world situation. The present study is part of a larger project designed to provide some further insights into the energy exchanges and conversions at the atmosphere/city interface, and thereby to provide more realistic input criteria for modelling.

The radiation balance for any surface is

$$Rn = (Q + q)(1 - \alpha) + I\downarrow - I\uparrow \qquad (1)$$

where, Rn – net surface all-wave radiation; Q, q – direct, and diffuse short-wave radiation; α – surface albedo; $I\downarrow$ – long-wave radiation emitted by the atmosphere (counter radiation); $I\uparrow$ – long-wave radiation emitted by the surface.

Some work is available regarding urban/rural $(Q+q)$ differences due to attenuation by urban pollutants (De Boer, 1966 for Rotterdam; East, 1968 for Montreal). The other term in Equation (1) which is determined by the nature of the atmosphere is $I\downarrow$. It is widely regarded that urban areas experience increased $I\downarrow$ due to atmospheric pollution, and that this is one of the causes of the urban heat island effect (Kratzer, 1956). On closer inspection this statement is found to be almost totally unsupported by observational evidence. Bach and Patterson (1969) report increased $I\downarrow$ over Cincinnati compared to a rural station. Unfortunately their results are from daytime observations using economical net radiometers, and the reported differences lie within the accuracy of these instruments. Terjung (1970) gives some intra-urban variations in radiant sky temperature over a small portion of Los Angeles, but no rural values are available for comparison, and the data are complicated by cloud. Yamamoto (1957), using a radiation chart, concluded that aerosols contribute $<1\%$ extra to $I\downarrow$ from unpolluted skies. In summary, therefore, we may conclude that there is a dearth of information regarding $I\downarrow$ for urban areas, and that available data are crude or in conflict.

The objective of this paper is to establish the reality and size of any urban increase in counter radiation, based on a direct measurement approach, employing accurate instrumentation. In addition, it is hoped to provide some information on the role of counter radiation in the production of the urban heat island, and in the urban surface energy balance. Observations are restricted to nights because then the radiation balance equation is abbreviated to the simple form:

$$Rn = I = I\downarrow - I\uparrow \tag{2}$$

where, I – net long-wave radiation. Because cloud would considerably confuse the $I\downarrow$ picture, only clear nights were used. In addition, the urban heat island effect attains its maximum intensity at night in Montreal (Oke and East, 1971) and this should maximize chances of establishing any links with $I\downarrow$.

2. Instrumentation

The observational programme involved the measurement of air temperature and atmospheric counter radiation, during automobile traverses across the Island of Montreal. The instrumentation was designed to yield high accuracy, even though combined with portability and fast response.

The radiation sensor was a polyethylene-shielded net radiometer (Swissteco Model S1) equipped with a uni-directional adaptor over the lower thermopile surface. In the absence of short-wave radiation at night, this arrangement provides an effective infrared pyrgeometer. The radiometer time constant was 23 s, and the thermopile output was $\simeq 0.39$ mV/mW cm^{-2}. The upper thermopile surface was covered by a moulded polyethylene dome, 0.5 mm in thickness. The dome was kept rigid by a controlled flow of dry-nitrogen at $\simeq 35$ ml min^{-1}, and a pressure of 0.30 kg cm^{-2}. This is stronger than the normal purging rate when the sensor is maintained at a static site. The extra strength was deemed necessary to prevent deformation of the dome when the automobile was in motion. Laboratory tests showed the sensor output to be insensitive to flow rate. The instrument is provided with ports for external ventilation, but this feature was not utilized due to the problems of operating a compressor in an automobile. In addition, it was felt that adequate ventilation to offset condensation or the settling of aerosols was provided by the motion of the vehicle.

The adaptor was an hemispheric black-body cavity whose inner surface temperature was continuously monitored with a copper-constantan thermocouple. The thermocouple was referenced to a thermostatically-controlled constant temperature bath. The adaptor responded to ambient temperature changes. This was acceptable since a continuous temperature record was kept, but it introduces problems in reducing the data. To offset this, the adaptor was embedded in a foam-rubber block and short-period fluctuations (<15 min) were eliminated. Counter radiation values were obtained by computing the cavity output via Stefan-Boltzmann's Law (assuming a cavity emissivity of unity), and subtracting this value from the instrument's total output.

The signals from both the thermopile and the cavity were continuously monitored on a potentiometric recorder (Honeywell Electronik 194). A portion of the thermocouple signal was bucked-out to allow use of sensitive recorder ranges.

Air temperature was measured with a small thermistor probe mounted in a shield made of polyvinyl-chloride tubing covered with reflective tape. The time constant of the probe was 0.5 s, and artificial aspiration was provided at a rate of 3.5 m s^{-1} by a small blower fan. A recording was registered every 0.25 s.

The net radiometer and temperature sensor were mounted on the roof of an automobile at $\simeq 1.5$ m (Figure 1). Since observations were taken with the car in motion,

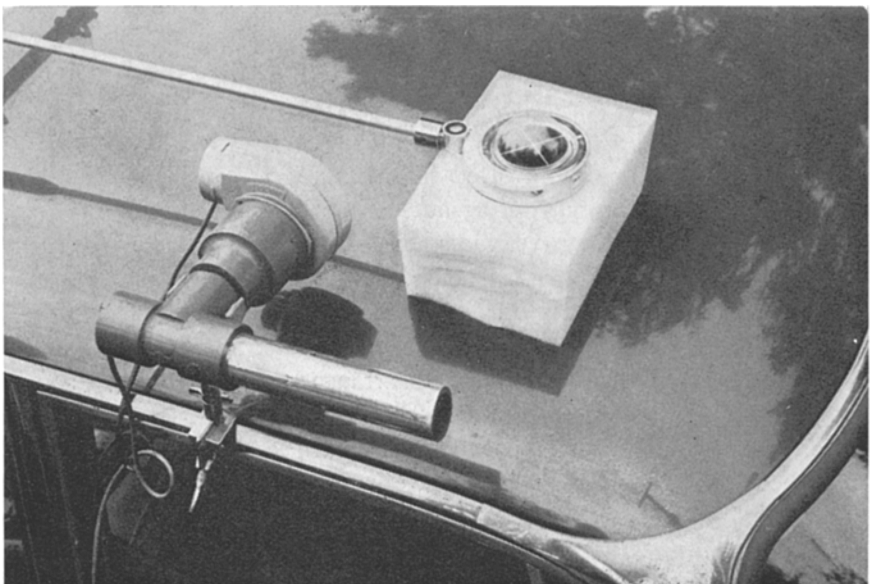

Fig. 1. Radiation and temperature sensors mounted on the automobile.

levelling of the radiometer could only be made before a traverse. However, the route was level, and since physical rocking of the car whilst stationary caused no discernible fluctuations in the trace, this error was assumed negligible. In general a constant speed of 50 km hr^{-1} was maintained during a traverse, but Table I shows that counter-radiation ($I\downarrow$) values are not seriously affected by the car's speed between 30 and 100 km hr^{-1}. Similarly, tests showed the air temperature measurements to be unaffected if speeds were <70 km hr^{-1}.

TABLE I

Effect of speed of automobile on $I\downarrow$ measurements

Speed (km hr^{-1})	<30	30–65	65–100	>100
$I\downarrow$* (mW cm^{-2})	0.998	1.000	1.004	1.006

$I\downarrow$* is the ratio of the value of $I\downarrow$ for the indicated speed range to the value for the speed range used in traverses (i.e., 30–65 km hr^{-1}).

Considering all the probable sources of error, it is considered that the absolute accuracy of the $I\downarrow$ observations is within 2.0 mW cm^{-2}, and that the relative accuracy within a particular traverse is $\leqslant 0.2$ mW cm^{-2}. Similarly, the air temperature data possess an absolute accuracy of 0.5 °C, and a relative accuracy of 0.2 °C.

3. Field Operations

The observation traverse route was arranged so as to completely cross the city of Montreal. The route, and the generalized land-uses of the Montreal region are shown in Figure 2. The main concentration of population (>1 million) is on the Island of Montreal, which is essentially flat except for Mount Royal (200 m), which is an isolated hill to the south-east of the traverse route. The downtown core lies between the St. Lawrence River and Mount Royal. The rest of the city is characterized by mixed commercial, light industrial and residential land-uses. The ribbon of industrial uses lies south and east of the traverse route, except in the north-east where it runs through a large complex of oil refineries.

The traverse route (Figure 2) followed highway 40, completely crossing the Island of Montreal along a south-west/north-east transect. Moving from the south-west, the traverse passed successively through rural, suburban, urban (commercial), suburban, industrial and back to rural land-uses. The portion of the route between Decarie Boulevard and Pie IX Boulevard is elevated to about 10 m. This is considered beneficial because this section contained the tallest buildings, which might otherwise have been in the radiometer's field of view. The route is a major 4–6 lane controlled-access freeway and hence buildings are set well back from the road, reducing view factor problems.

Each traverse consisted of two complete transects of the route in opposite directions. The recorder traces were annotated *en route* and additional descriptive comments were tape-recorded. (As an interesting practical note, the radiation trace provided its own

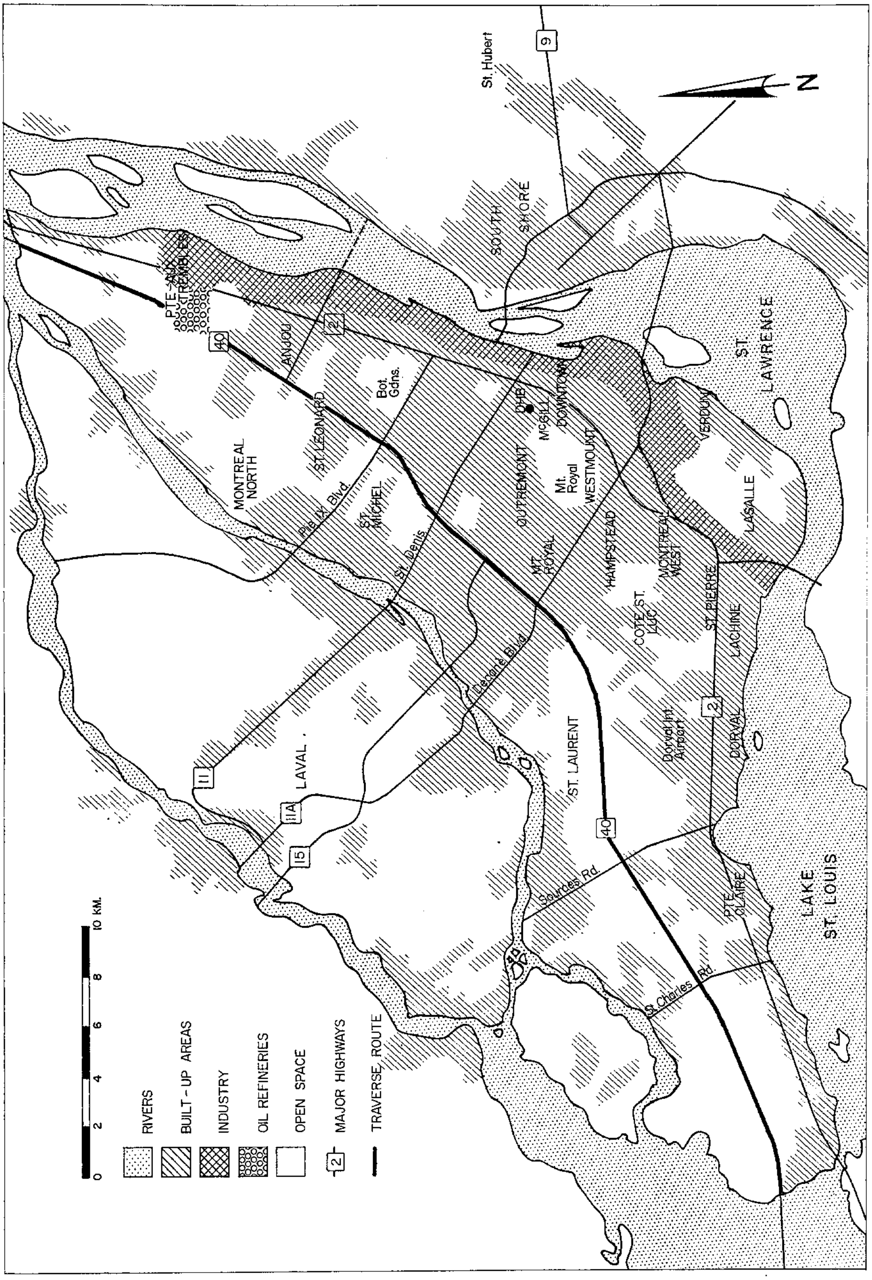

Fig. 2. Location and land-use map of Montreal including the traverse route.

event marks as sudden 'spikes' in the signal, due to travelling under overpasses which radiate strongly.) By maintaining a constant speed, and assuming that both air temperature and $I\downarrow$ varied linearly with time, it was possible to average the data for any location and obtain results which were standardized to the mid-time of the traverse period. A typical traverse period was about 90 min. Only those traverses which showed $<5\%$ variation in $I\downarrow$ values between the outward and inward legs are presented here.

4. Traverse Observations

Counter-radiation ($I\downarrow$) and temperature (T) traverses were conducted simultaneously during the period August 1969 to July 1970; two were during the winter and the rest in the spring and summer months. Twelve traverses satisfied the steady-state conditions mentioned above, and a summary of the data and the prevailing meteorological and pollution conditions is given in Table II.

Figure 3 (a–c) shows a comparison of traverse results from three nights during June 1970. In this and following figures, the traverse route has been projected onto a straight line. This slightly exaggerates gradients of the measured parameters between St. Charles Road and Decarie Boulevard. With respect to cloud, wind direction and water vapour pressure, these nights are almost identical, but it will be noted (Table II) that wind speeds vary from 0.4 to 5.0 m s^{-1}.

The $I\downarrow$ and T profiles across the city parallel each other very closely on each occasion. Both parameters show a marked increase from a rural 'background' level immediately upon encountering the built-up area, at the so-called heat-island 'cliff'. Both $I\downarrow$ and T peak at approximately the same location which is always within the urban area. Finally, both parameters decrease in value downwind of the urban centre, but the $I\downarrow$ values do not always appear to assume immediately their upwind rural levels, especially with good ventilation (e.g., Figure 3(a)).

In the following analyses, we will refer to urban/rural comparisons of a number of meteorological parameters. These will be indicated as a finite difference of the variable's highest urban, and lowest upwind rural values (e.g., ΔT_{u-r} is the urban heat-island intensity). In Figure 3 (a–c) and Table II, it is evident that for the illustrated three June days, as the wind speed ($\bar{u}$) decreases from 5.0 to 0.4 m s^{-1}, the values of ΔT_{u-r} increase from 2.2 to 7.0°C, and $\Delta I\downarrow_{u-r}$ increases from 0.7 to 4.0 mW cm^{-2}.

Figure 4 shows the traverse for February 15, 1970, one of the winter runs. Winds were SE 0.8 m s^{-1}, skies were clear, air temperatures very low ($\simeq -20$°C), and water vapour pressures correspondingly small ($\simeq 1$ mb). The urban heat island was impressively displayed, with $\Delta T_{u-r} = 9.5$°C (further information on this case, including urban/rural cooling rates and the temporal variation of ΔT_{u-r}, is given in Oke and East, 1971). On this occasion the $I\downarrow$ profile parallels the T profile across the route until it reaches the downwind urban/rural boundary where there is an even larger peak in $I\downarrow$ than that found in the city centre. It is felt that this apparent anomaly in the general pattern described above is due to the oil refinery complex. The main part of this complex lies to the south-east of the traverse route, and so a wind from this sector

TABLE II

Summary of traverse and general meteorological data

Date	Time[a] (EST)	$\bar{u}$[b] (m s^{-1})	Cloud[b]	e[c] (mb)	COH[d]	ΔT_{u-r}[e] (°C)	$\Delta I{\downarrow}_{u-r}$[e] (mW cm^{-2})	$\Delta I{\downarrow}_{u-r}$[f] % increase
Aug. 12 1969	2140	SW 2.7	0	16.9	0.7	3.6	1.5	4.5
Oct. 30 1969	0100	N 1.8	0	3.9	1.2	4.5	1.2	5.4
Feb. 15 1970	0030	SE 0.8	0	1.3	1.4	9.5	4.0	25.3
May 23 1970	2200	W 3.0	AC 1	9.9	0.6	1.6	0.7	2.4
May 28 1970	2110	SW 1.8	0	7.9	0.9	3.7	1.2	4.0
June 8 1970	2140	S 2.0	Ci 1	16.0	0.7	3.4	1.1	3.1
June 9 1970	2045	SW 5.0	0	16.0	0.6	2.2	0.7	2.0
June 14 1970	2140	SSW 3.5	Ci 1	9.8	0.7	4.0	1.7	5.3
June 16 1970	2315	W 0.4	0	16.1	1.2	7.0	4.0	13.2
June 22 1970	2100	WSW 6.2	AC 1	12.9	0.4	1.8	0.6	1.8
June 25 1970	2100	W 2.6	SC 1	9.5	0.5	2.1	1.3	4.5
June 28 1970	2150	SW 4.5	0	11.0	0.5	1.1	0.6	1.9

[a] Mid-time of traverse.
[b] Average wind at Dorval.
[c] Vapour pressure at McGill Observatory.
[d] Average coefficient of haze of 3 urban stations along the traverse.
[e] Using highest urban and lowest upwind rural values.
[f] $\Delta I{\downarrow}_{u-r}/I{\downarrow}_r \times 100$.

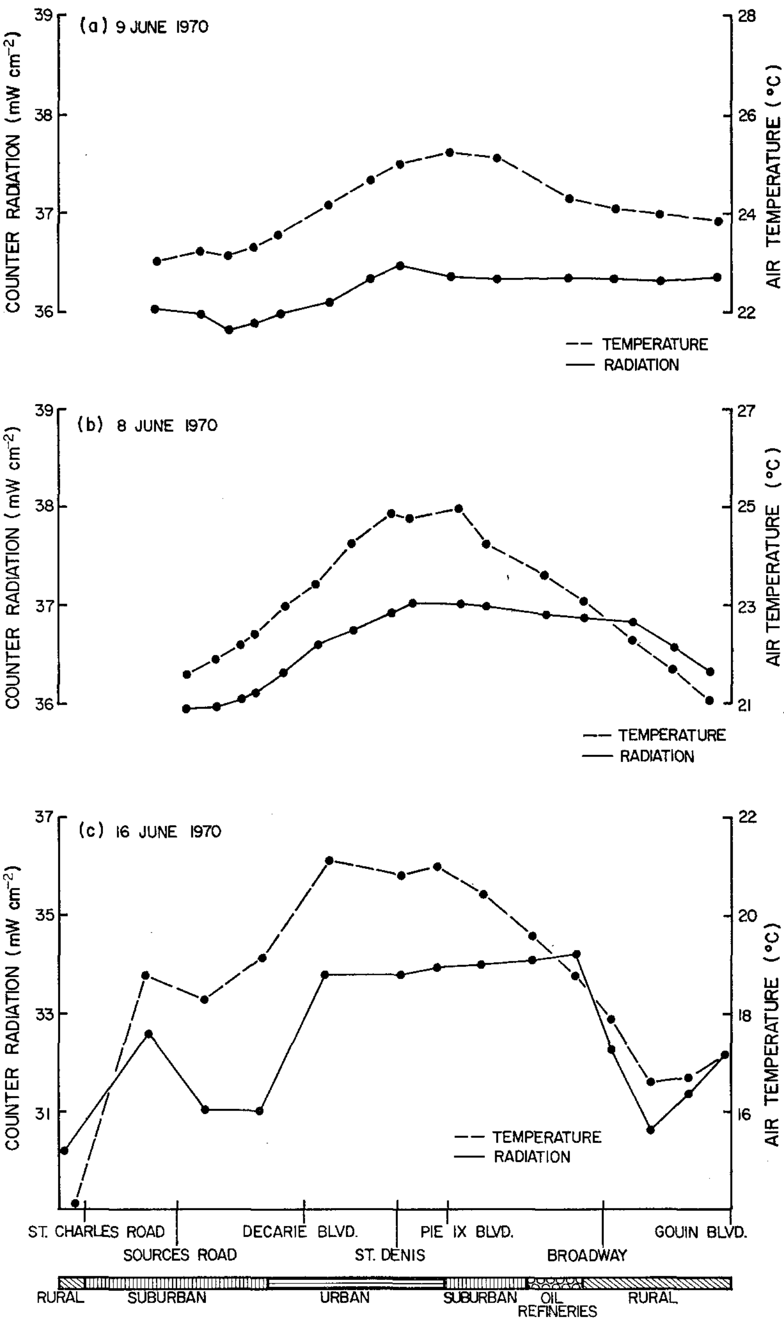

Fig. 3a–c. Counter radiation and air temperature profiles across Montreal for (a) June 9, 1970, wind SW 5.0 m s^{-1}, (b) June 8, 1970, wind S 2.0 m s^{-1}, and (c) June 16, 1970, wind W 0.4 m s^{-1}.

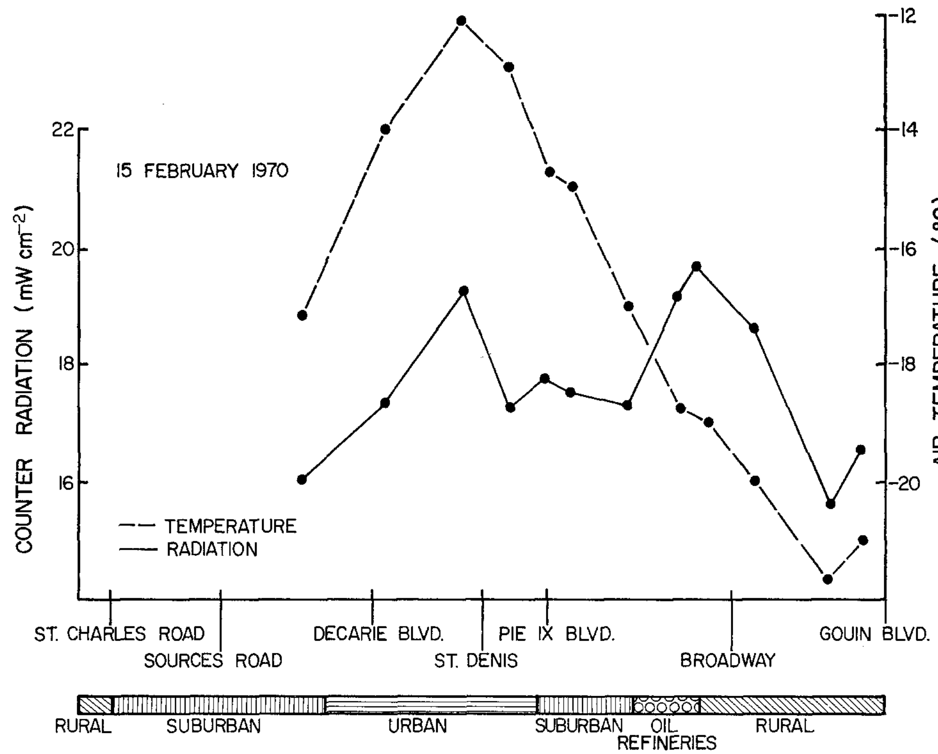

Fig. 4. Counter radiation and air temperature profile across Montreal for February 15, 1970, wind SE 0.8 m s^{-1}.

carries considerable effluent across the observation route. During the winter, this plume effect is likely to be most marked on $I\downarrow$ because the saturation vapour pressure is so low that water vapour almost immediately condenses into dense cloud after leaving the stacks, thus producing a very effective infra-red black-body absorption and emission layer at about 200 m. In addition, the temperature difference between the ground and the stack gases is at a maximum in winter, and hence the radiation exchange between them is also at a maximum. Similarly, the other winter run with low temperatures and humidities showed a peak in the same area. In summer with light winds (Figure 3(c)), $I\downarrow$ is again seen to show an increase in the oil refinery area, but the peak is less pronounced.

From the foregoing it seems certain that an urban area such as Montreal does receive an increase in counter radiation, at least at night. The urban/rural increases, $(\Delta I\downarrow_{u-r})$, may be as great as 4.0 mW cm^{-2} ($\simeq$0.057 cal cm^{-2} min^{-1}), and this could represent as much as a 25% increase over rural values. However, these are extremes, and an increase of 1 to 2 mW cm^{-2} ($\simeq$0.014 to 0.028 cal cm^{-2} min^{-1}) appears more representative (Table II). The following section discusses the relation between this increase in $I\downarrow$ and atmospheric parameters which might be expected to be related.

5. Urban/Rural Counter Radiation Differences

Having established that $I\downarrow$ is greater in the urban area, a physical cause must be sought. This study was not originally designed to answer this question, but the following discussion may provide some insight into the problem.

Essentially we are concerned with the question whether the observed urban increase in $I\downarrow$ is due to an increase in the emissivity of the urban atmosphere, or whether it is simply due to the increase in urban air temperature. The former could be the result of a change in the atmospheric constituents which affect the exchange of long-wave radiation (e.g., water vapour, aerosols or gases). The latter could be due to non-radiative warming of the atmosphere through the turbulent sensible heat flux drawing upon artificial heat generation and stored heat, in the city.

First of all we may consider simple scatter plots of $\Delta I\downarrow_{u-r}$ versus pollution (COH), heat-island intensity (ΔT_{u-r}) and wind speed ($\bar{u}$) as shown in Figure 5(a–c). All three parameters show recognizable relationships to $\Delta I\downarrow_{u-r}$, but statistical correlations were not performed due to the small numbers of data points, and because the sample population is not normally distributed with respect to $\Delta I\downarrow_{u-r}$.

It appears that as the COH value increases, so does $\Delta I\downarrow_{u-r}$. The same type of response is even more clearly defined for ΔT_{u-r}, and as the heat island becomes negligible ($<1\,°C$), so do counter-radiation differences. These scatter plots do not, however, help resolve the question of causation, and Figure 5(c) helps explain why. Wind speed exerts a strong influence on both COH and ΔT_{u-r} (see Table II), the former through its effect on diffusion, and the latter via advection.

The question of causation may, however, be studied by comparing the observed $I\downarrow$ values with those computed from empirical relations. The equations used were those of Ångström (1916), Brunt (1932), Swinbank (1963) and Idso and Jackson (1969). The equations and their constants are given in Table III. It will be noted that the Ångström and Brunt equations require both air temperature and humidity at screen-level, whereas the Swinbank and Idso and Jackson equations require only temperature measurements. In this study the 1.5-m traverse temperatures, and the McGill Obser-

TABLE III

Empirical equations used to calculate $I\downarrow$ for clear skies (T in °K, e in mb, $I\downarrow$ in mW cm^{-2})

Author	Equation	Constants
Ångström (1916)	$I\downarrow = \sigma\varepsilon T^4[a - b\exp(-2.3\,ce)]$	$a = 0.82$ $b = 0.25$, $c = 0.94$[a]
Brunt (1932)	$I\downarrow = \sigma\varepsilon T^4(a + b\sqrt{e})$	$a = 0.604$ $b = 0.048$[b]
Swinbank (1963)	$I\downarrow = 9.35 \times 10^{-6}\,\sigma\varepsilon T^6$	
Idso and Jackson (1969)	$I\downarrow = \sigma\varepsilon T^4\{1 - c\exp[-d(273 - T)^2]\}$	$c = 0.261$ $d = 7.77 \times 10^{-4}$

[a] Following Morgan *et al.* (1970)
[b] Following Sellers (1965).

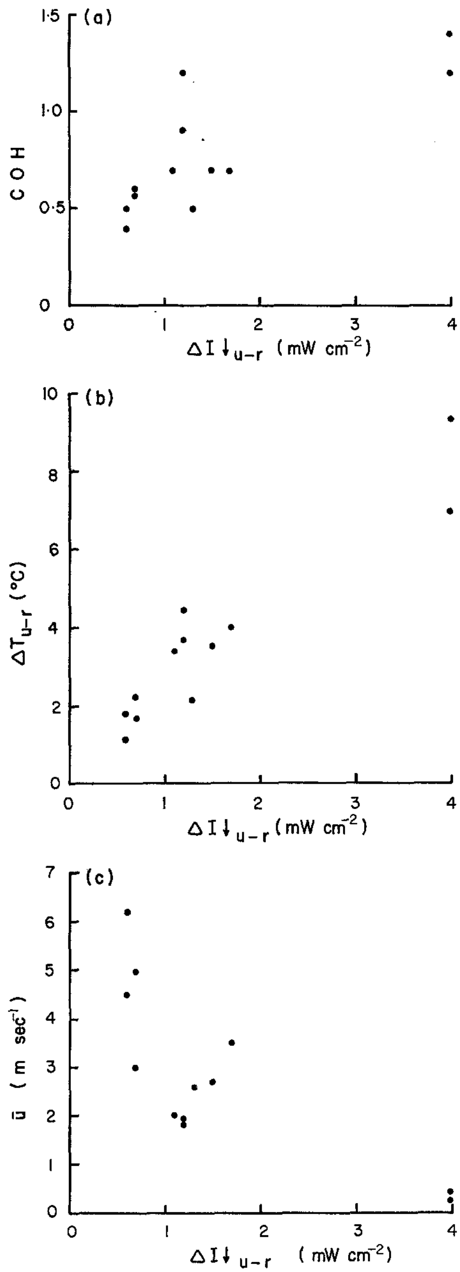

Fig. 5a–c. Urban/rural counter radiation differences versus (a) COH, (b) urban heat island intensity and (c) wind speed in the Montreal region.

vatory (Figure 2) vapour pressure observations were used in the absence of traverse humidities. Analysis of the Dorval (rural) and McGill (urban) vapour pressure readings showed that between 1900 and 0100 EST, urban/rural differences were <2 mb. The maximum error in computed $I\downarrow$ using *only* McGill data was found to be

0.24 mW cm^{-2} at 25 °C and 20 mb, and 0.25 mW cm^{-2} at 0 °C and 5 mb. These errors are approximately equivalent to instrumental errors and were considered acceptable. The empirical coefficients were not adjusted to provide a 'best-fit' between observed and calculated values for the Montreal area. Similarly no corrections were applied for the small amounts of Cirrus clouds observed on some nights (Table II).

Figure 6 shows a typical plot of the measured and calculated $I\downarrow$ values. From this and from data obtained on other nights, it was concluded that the empirical methods gave results usually within 5% of the measured values. The Ångström equation consistently underestimated in both urban and rural areas, whereas the other three equations tended to underestimate in rural areas but approximate or overestimate in the urban area.

The real significance, however, lies not in the agreement between the measured and calculated values of $I\downarrow$, but in the trend of their differences. Figure 7(a–c) shows the differences between measured and calculated values for the three nights illustrated in Figure 3, using one empirical method requiring both temperature and vapour pressure (Brunt), and one requiring temperature alone (Idso and Jackson). (There is no special significance in this choice.) It should be noted that the *absolute* error in obtaining both calculated and observed values of $I\downarrow$ exceeds their difference and therefore the sign has no significance. However, the *relative* error between values on the same traverse is an order of magnitude smaller than their differences, therefore urban/rural variations are real and significant. Again it is important to stress that the absolute

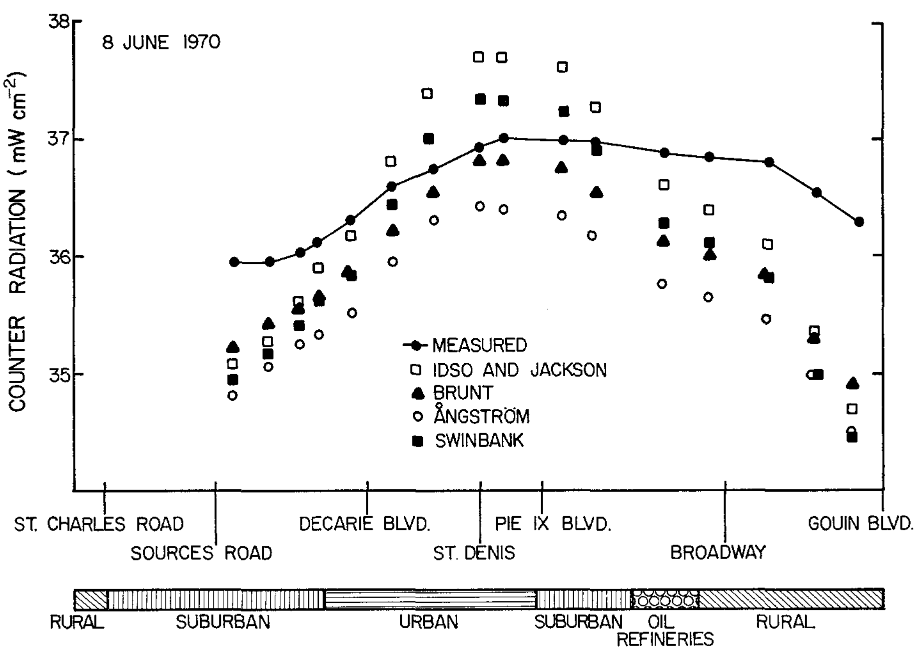

Fig. 6. Comparison of measured counter radiation across Montreal with that calculated from the Ångström, Brunt, Swinbank and Idso and Jackson empirical methods, for June 8, 1970.

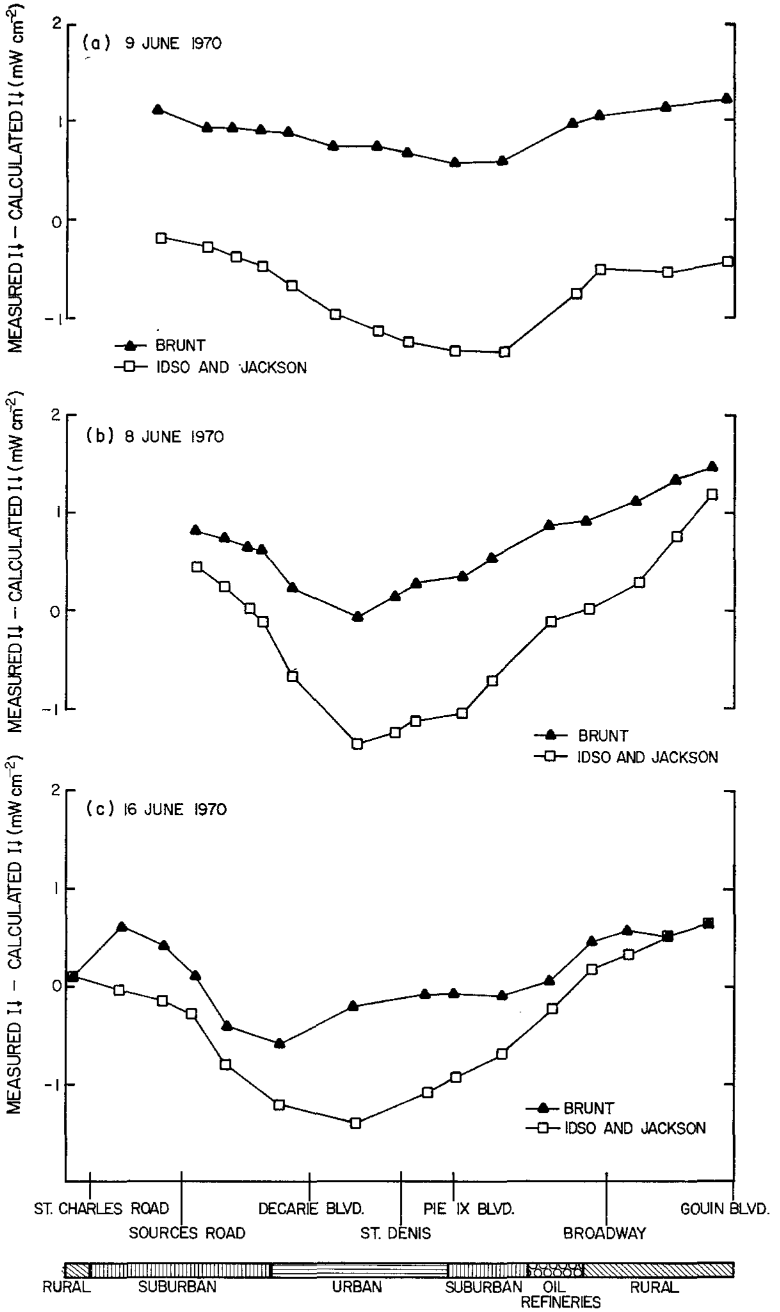

Fig. 7a–c. Profiles of the difference between measured counter radiation and that computed according to Brunt, and Idso and Jackson for (a) June 9, 1970, (b) June 8, 1970, and (c) June 16, 1970.

agreement between the two methods, or the agreement between the predicted and observed values is not particularly important. What is important is that each difference curve shows a dip which coincides with the urban area. This feature was found on almost all occasions. This dip indicates that the urban area receives less counter radiation relative to the rural area than to be expected on the basis of calculations from surface temperature variations. This decrease is of the order of 1 to 2 mW cm^{-2}.

Considering the nature of the empirical equations, one, or both of two features of the atmosphere could account for this apparent decrease in calculated $I\downarrow$ for the urban area. Either the urban atmosphere has a lower emissivity than that in the country, or the vertical temperature structure is considerably different between the two areas. These two possibilities are explored further below.

It seems highly improbable that the addition of pollutants to the urban atmosphere would decrease its emissivity. Theoretical analyses by Yamamoto (1957) and Zdunkowski *et al.*, (1966) indicate that the effects of smoke and haze are small, but that they will tend to increase rather than decrease sky emissivities. Similarly Möller (1951), Monteith (1961) and Atwater (1971) have all argued that air pollution will produce an increase in $I\downarrow$. Inversely it might be argued that a reduction of water vapour in the city could produce a lowered atmospheric emissivity. This, however, is contrary to the observations of Chandler (1962, 1967) in London and Leicester, and Ackerman (1970) in Chicago, which all show slightly higher amounts of water vapour in the urban areas. In addition, it can be quantitatively shown that a 10 mb urban/rural vapour pressure difference is required to produce the 2 mW cm^{-2} difference in $I\downarrow$. This grossly exceeds any reported urban/rural humidity differences, and does not agree with the Dorval-McGill analysis reported above.

On the other hand, the reported urban/rural differences in vertical temperature structure provide a plausible and sufficient explanation for the calculated decrease in sky emission over the urban area. The recent studies of Bornstein (1968) for New York, Clarke (1969) for Cincinnati and of special interest in this study, Yap *et al.* (1969), and Oke and East (1971) for Montreal have shown a similarity in urban/rural profile forms on clear nights. Characteristically the rural areas show surface-based inversions, whereas the urban area exhibits adiabatic or weak lapse profiles within a shallow (200-300 m) urban boundary layer. In Montreal this urban mixing layer often exhibits a lapse rate of $-6\,^{\circ}\mathrm{C\,km^{-1}}$. The effect of a rural inversion is to provide a warmer radiating atmosphere aloft which will give greater $I\downarrow$ than predicted from surface temperatures. Conversely, the urban lapse profile provides a cooler atmosphere aloft, thus decreasing $I\downarrow$ compared to that expected from surface temperature observations.

Möller (1951) has shown that variations in temperature gradient are capable of producing marked differences in $I\downarrow$ from clear skies. Table IV shows that the $I\downarrow$ difference between an urban lapse profile and a rural inversion profile is almost exactly the same as that needed to match the measured and computed $I\downarrow$ values in Montreal, and in its upwind rural area. This reasoning also explains why downwind rural differences between measured and calculated $I\downarrow$ were often greater than upwind rural differences (e.g., Figure 7(b) and (c)). In the downwind area when the surface temperatures drop and a surface-based inversion begins to develop, an 'urban plume' lies overhead (Clarke 1969). This elevated warm layer will augment the value of $I\downarrow$ and hence the underestimation based on cool surface temperatures.

TABLE IV

The effect of the vertical temperature distribution on $I\downarrow$ (after Möller, 1951)

Inversion thickness (m)	Temperature increase (°C)	$I\downarrow$[a] (mW cm^{-2})	Difference from lapse of 6°C km^{-1} (mW cm^{-2})
100	9.4	25.11	1.81
200	8.8	24.83	1.53
300	8.2	24.62	1.33
400	7.6	24.48	1.18
500	7.0	24.41	1.11
1000	0.0	23.99	0.70
	6°C km^{-1}	23.29	0.00
Lapse rate	Adiabatic	23.23	−0.06

[a] Based on a surface temperature of 0°C, and a total water vapour path of 1.12 g cm^{-2}.

The above analysis therefore shows that the role of pollutants and water vapour is probably not as important as the modification of the vertical temperature structure in contributing to an increase in $I\downarrow$ over the urban area. Indeed the numerical analysis of Atwater (1971), and the infra-red flux divergence measurements of Fuggle (1971), both indicate that the role of pollutants is to cool rather than to warm the atmosphere, and would thus serve to decrease rather than increase the value of $I\downarrow$ in an urban atmosphere. It would appear, therefore, that counter radiation does not result from an increase in emissivity in polluted air and therefore does not represent a source of energy preferentially found in the city. As such, the observed increase in $I\downarrow$ is probably an effect rather than a cause of the urban heat island. Certainly, based on the calculations of Oke and East (1971), the energy necessary to support the modification of the urban boundary layer is at least 10 times greater than the observed 1 to 2 mW cm^{-2} increase in $I\downarrow$, even if it were considered to be a uniquely urban phenomenon.

6. Urban/Rural Net Radiation Differences

Using the measured $I\downarrow$ values as a base, it is possible to arrive at some preliminary estimates of the net long-wave radiative exchanges in Montreal and the upwind rural areas. Since at night the net long-wave radiation (I), represents the net all-wave radiative exchange (Rn), (Equation (2)), this allows some insight into the possibility of using urban/rural differences to infer the basic radiative component of the surface energy balance.

Table V presents the components of the long-wave radiation balance for both the urban and rural areas in and around Montreal for the nights on which traverses were

TABLE V

Nocturnal urban/rural long-wave radiation components (mW cm^{-2})

Date	$I{\downarrow}_u$	$I{\downarrow}_r$	$\Delta I{\downarrow}_{u-r}$[a]	$I{\uparrow}_u$	$I{\uparrow}_r$	$\Delta I{\uparrow}_{u-r}$[a]	$I_u = Rn_u$	$I_r = Rn_r$	$\Delta I_{u-r} = \Delta Rn_{u-r}$[a]
Aug. 12 1969	34.9	33.4	+1.5	−43.9	−41.8	+2.1	− 9.0	−8.4	+0.6
Oct. 30 1969	23.4	22.2	+1.2	−32.0	−30.1	+1.9	− 8.6	−7.9	+0.7
Feb. 15 1970	19.8	15.8	+4.0	−26.7	−22.8	+3.9	− 6.9	−7.0	−0.1
May 23 1970	29.6	28.9	+0.7	−39.6	−38.8	+0.8	−10.0	−9.9	+0.1
May 28 1970	31.1	29.9	+1.2	−39.2	−37.2	+2.0	− 8.1	−7.3	+0.8
June 8 1970	37.0	35.9	+1.1	−45.0	−43.0	+2.0	− 8.0	−7.1	+0.9
June 9 1970	36.5	35.8	+0.7	−45.2	−43.9	+1.3	− 8.7	−8.1	+0.6
June 14 1970	33.5	31.8	+1.7	−42.7	−40.4	+2.3	− 9.2	−8.6	+0.6
June 16 1970	34.2	30.2	+4.0	−42.7	−38.8	+3.9	− 8.5	−8.6	−0.1
June 22 1970	33.7	33.1	+0.6	−42.6	−41.6	+1.0	− 8.9	−8.5	+0.4
June 25 1970	30.1	28.8	+1.3	−39.7	−38.6	+1.1	− 9.6	−9.8	+0.2
June 28 1970	31.9	31.3	+0.6	−41.4	−40.8	+0.6	− 9.5	−9.5	0.0
Average	31.3	29.8	+1.5	−40.1	−38.2	+1.9	− 8.8	−8.4	+0.4

[a] Positive values indicate that the urban value (loss or gain) is greater than the rural value.

conducted. The chosen points represent the maximum or minimum values in each case (e.g., the lowest upwind $I{\downarrow}_r$, and the highest $I{\downarrow}_u$). The $I{\downarrow}_u$, $I{\downarrow}_r$ and $\Delta I{\downarrow}_{u-r}$ values were measured. Using the traverse temperature data, $I{\uparrow}_u$, $I{\uparrow}_r$ and $\Delta I{\uparrow}_{u-r}$ values were computed using the simple Stefan-Boltzmann relation. In doing so it was necessary to assume that urban and rural emissivities were the same and equal to unity, and that the 1.5-m air temperature approximated that at the surface. The advisability of employing these assumptions is considered later. Having the above values, I_u, I_r and ΔI_{u-r} were easily obtained.

The individual $I{\downarrow}_u$ and $I{\downarrow}_r$ values show a considerable range due to ambient temperatures, but as noted previously their differences consistently show an increased receipt of radiation in the city. Similarly $I{\uparrow}$ values show a variation due to absolute temperatures, and because $\Delta I{\uparrow}_{u-r}$ is proportional to ΔT_{u-r}, $I{\uparrow}$ always shows a greater loss for the warmer urban area at night. The difference lies between 0.6 and 3.9 mW cm^{-2}. The net radiative loss terms for both environments show little variability ranging only from 6.9 to 10.0 mW cm^{-2}.

The most important result of this analysis is the very small ΔI_{u-r} difference exhibited between the urban and rural areas. On two occasions the rural area shows a very slightly higher radiative loss; the remaining cases show a very slightly larger urban deficit. The greatest urban/rural difference is only 0.9 mW cm^{-2} ($\simeq$0.01 cal cm^{-2} min^{-1}), and the average is 0.4 mW cm^{-2} (0.006 cal cm^{-2} min^{-1}).

It is important at this juncture to consider further the nature of the assumptions used in this development. The similarity of urban/rural emissivities remains largely unproven. However, on the basis of previous assessments for concrete and other building materials, and for typical rural surfaces (Sellers, 1965), the indications are that emissivities are not radically dissimilar. This is supported by measurements in Columbia, Maryland (Landsberg, 1971, personal communication). The city may possess a slightly lower emissivity and this would serve to bring urban/rural values even closer, rather than accentuate differences. Considering the assumption that $T_{1.5} = T_0$, if one assumes a reasonable rural temperature difference between the surface and 1.5 m, on a clear night with weak winds, to be 2°C (e.g., Oke 1970), then $I{\uparrow}_r$ will be overestimated by <1 mW cm^{-2}. In the city with the weak lapse conditions already noted, $I{\uparrow}_u$ may be very slightly increased. Both of these errors, however, will be reduced at higher wind speeds due to mixing, and it therefore seems unlikely that the figures in Table V will be radically affected. The analysis therefore indicates that the increase in $I{\downarrow}$ in the urban area is real, but is completely offset by the increased $I{\uparrow}$ from the warmer urban surface. This tends to substantiate the view that urban/rural radiation differences are unlikely to alter surface energy balance comparisons radically at night. This view, however, must await vindication through direct measurement of urban/rural net radiation differences. When taking such measurements, one must be careful to choose 'representative' sites, and one must include temporal variations in ΔI_{u-r} since all the traverses presented here were conducted at the time when Montreal's urban heat island is usually at its maximum (Oke and East, 1971). Measurements during the early evening, when ΔT_{u-r} is developing, would therefore be particularly helpful.

7. Conclusion

The results of this study indicate that a large urban area does receive a greater amount of long-wave radiation from the atmosphere at night in comparison with that received by a rural area upwind. This increase is still prevalent downwind of the city. It appears, however, that the increase is due to the increased warmth of the city atmosphere rather than to any change in the radiative properties of the atmosphere such as is often attributed to the pollution 'blanket'. Increased counter radiation cannot therefore be construed to be a cause of the heat island; rather it is the result of an atmosphere which is warmed by other means.

Although the results indicate only small changes in counter radiation due to urban effects, they do indicate that man-made, thermal, gaseous, and particulate pollution of the atmosphere can influence the infra-red radiation balance at the surface. It would be interesting, for example, to determine how many kilometres downwind the 'plume' effect continues. As urbanization proceeds, these ramifications will increasingly assume global importance.

The consideration of urban/rural net radiation differences shows a remarkably small difference in available radiant energy at the surface at night. Indeed, instead of the urban area showing a preferential radiative gain, on most occasions the city exhibits a deficit. Presumably therefore, our investigations regarding heat-island causation should concentrate more deeply upon eddy heat flux, storage and space-heating considerations.

These results tend to support the assumption that long-wave radiation can be omitted in the development of certain heat-island models (e.g., Summers, 1964; Myrup, 1969). However, the conclusions should not be construed as relegating long-wave exchanges to a minor role in the *atmospheric* energy balance, nor should the small *net* radiation differences be allowed to mask important changes in the size and nature of each *component* flux.

Acknowledgements

This research was supported by grants from the Canadian Meteorological Service, and the National Research Council of Canada, to whom grateful acknowledgements are extended.

Thanks are also due to Mr P. Hitschfeld for help in conducting traverses; to the National Atmospheric Radiation Centre, Canadian Meteorological Service, Toronto, for radiometer calibrations; and to the Health Department of the City of Montreal for providing air pollution data.

References

Ackerman, B.: 1970, 'Urban-rural Differences in the Temperature and Dew Point in the Chicago Area', Argonne National Lab. Radiol. Phys. Div. Annual Report, ANL 7760.

Ångström, A.: 1916, 'Uber der Gegenstrahlung der Atmosphäre', *Meteorol. Zeitsch.* **33**, 529–38.

Atwater, M. A.: 1971, 'The Radiation Budget for Polluted Layers of the Urban Environment', *J. Appl. Meteorol.* **10**, 205–14.

Bach, W. and Patterson, W.: 1969, 'Heat Budget Studies in Greater Cincinnati', *Proc. Assoc. Amer. Geographers* **1**, 7–11.

Bornstein, R. D.: 1968, 'Observations of the Urban Heat Island Effect in New York City', *J. Appl. Meteorol.* **7**, 575–82.
Brunt, D.: 1932, 'Notes on Radiation in the Atmosphere', *Quart. J. Roy. Meteorol. Soc.* **58**, 389–420.
Chandler, T. J.: 1962, 'Temperature and Humidity Traverses across London', *Weather* **17**, 235–42.
Chandler, T. J.: 1967, 'Absolute and Relative Humidities in Towns', *Bull. Amer. Meteorol. Soc.* **48**, 394–9.
Clarke, J. F.: 1969, 'Nocturnal Urban Boundary Layer over Cincinnati, Ohio', *Monthly Weather Rev.* **97**, 582–9.
De Boer, H. J.: 1966, 'Attenuation of Solar Radiation due to Air Pollution in Rotterdam and its Surroundings', Koninklijk Nederlands Meteorologisch Instituut, Wetenschappelijk Rapport W.R. 66–1, 36 pp.
East, C.: 1968, 'Comparaison du Rayonnement Solaire en Ville et à la Campagne', *Cah. de Geog. de Quebec* **12**, 81–9.
Fuggle, R. F.: 1971, 'Nocturnal Atmospheric Infrared Radiation in Montreal', Ph.D. Thesis, McGill University, Montreal, 237 pp.
Idso, S. B. and Jackson, R. D.: 1969, 'Thermal Radiation from the Atmosphere', *J. Geophys. Res.* **74**, 5397–403.
Kratzer, P.: 1956, *Das Stadtklima*, Friedrich Vieweg und Sohn, Braunschweig, 221 pp.
Möller, F.: 1951, 'Long-wave Radiation', in *Compendium of Meteorology*, Amer. Meteorol. Soc., Boston, 34–49.
Monteith, J. L.: 1961, 'An Empirical Model for Estimating Long-wave Radiational Exchanges in the British Isles', *Quart. J. Roy. Meteorol. Soc.* **87**, 171–9.
Morgan, D. L., Pruitt, W. O., and Lourence, F. J.: 1970, 'Radiation Data and Analyses for the 1966 and 1967 Micrometeorological Field Runs at Davis, California', Tech. Report ECOM 68-G10-2, Dept. Water Sci. and Eng., Davis, Calif., 45 pp.
Myrup, L. O.: 1969, 'A Numerical Model of the Urban Heat Island', *J. Appl. Meteorol.* **8**, 908–18.
Oke, T. R.: 1970, 'The Temperature Profile near the Ground on Calm Clear Nights', *Quart. J. Roy. Met. Soc.* **96**, 14–23.
Oke, T. R. and East, C.: 1971, 'The Urban Boundary Layer in Montreal', *Boundary-Layer Meteorol.* **1**, 411–37.
Sellers, W. D.: 1965, *Physical Climatology*, Univ. of Chicago Press, 272 pp.
Stern, A. C.: 1970, 'Utilization of Air Pollution Models', in Proceedings of Symposium on Multiple Source Urban Diffusion Models (Stern, A.C., Ed.), U.S. Environmental Protection Agency, AP-86, 13.1–13.8.
Summers, P. W.: 1964, 'An Urban Ventilation Model Applied to Montreal', Ph.D. Thesis, McGill Univ., Montreal.
Swinbank, W. C.: 1963, 'Longwave Radiation from Clear Skies', *Quart. J. Roy. Meteorol. Soc.* **89**, 339–48.
Terjung, W. H.: 1970, 'Urban Energy Balance Climatology: a Preliminary Investigation of the City-Man System in Downtown Los Angeles', *Geog. Rev.* **60**, 31–53.
Yamamoto, G.: 1957, 'Estimation of Additional Downward Radiation from Aerosols over Large Cities', *J. Meteorol. Soc. Japan*, 75th Anniversary Volume, 1–4.
Yap, D., Gunn, K. L., and East, C.: 1969, 'Vertical Temperature Distribution over Montreal', *Naturaliste Can.* **96**, 561–80.
Zdunkowski, W., Henderson, D., and Hales, J. V.: 1966, 'The Effect of Atmospheric Haze on Infra-red Radiative Cooling Rates', *J. Atmos. Sci.* **23**, 297–304.